Engineering and Technology Journal e-ISSN: 2456-3358

Volume 09 Issue 08 August-2024, Page No.- 4893-4897

DOI: 10.47191/etj/v9i08.39, I.F. – 8.227

Synthesis of Acid Co-Precipitated WO_3 Nanoflowers and Its Characterization: Structural, Optical, and Morphological Insights

Ashna Verma[1], Shreya[2], Peeyush Phogat[3], N.L. Singh[4], Ranjana Jha[5]

[1,2,3,4,5]Research lab for Energy Systems, Department of Physics, Netaji Subhas University of Technology, New Delhi- 110078, India

ABSTRACT: In the current research, we delve into the synthesis and comprehensive characterization of tungsten oxide (WO_3) nanostructures, unveiling novel insights that promise advancements in various technological realms through a facile acid co-precipitation method. The obtained material underwent characterization employing a variety of analytical methods, including X-ray diffraction, UV-Vis spectroscopy, and scanning electron microscopy. X-ray diffraction was employed to elucidate the crystallographic details, identify different phases, and estimate crystallite size and microstrain values using the Williamson-Hall plot and Debye-Scherer method. A band gap of approximate 2.5 eV was determined through the analysis of UV-Vis spectroscopy, along with the assessment of additional optical properties such as absorbance range, refractive index, and HOMO-LUMO levels. The morphological investigation using FESEM images revealed the formation of nanosheets arranged in a flower-like structure. Therefore, our investigation demonstrated that the as- synthesized tungsten oxide (WO_3) exhibits promising properties, showcasing excellent outcomes in optical, structural, and morphological analyses. Notably, the results indicate highly favourable characteristics for various applications, paving the way for their utilization in efficient and sustainable energy conversion systems.

KEYWORDS: Acid co-precipitation, Nanoflowers, nanosheets, Tungsten oxide

1. INTRODUCTION

In the rapidly evolving realm of contemporary science and technology, the persistent and ever-growing global demand for energy necessitates exploration and innovation in search of new approaches. There is an urgent call for environmentally conscious solutions to address this pressing need. Amidst this pursuit, innovative and sustainable materials have emerged as crucial contributors. These materials are designed to harness natural processes and renewable resources to mitigate environmental impact. By focusing on efficiency and cost-effectiveness, these advanced technologies are paving the way for significant strides in pollution reduction, energy conservation, and waste management. The development and implementation of these materials are essential in our collective effort to create a cleaner and more eco-friendly future. Through continued research and collaboration, we can accelerate the adoption of these green technologies, ensuring a healthier planet for generations to come. Researchers are actively exploring green materials, innovative manufacturing processes, and recycling methods to minimize the environmental impact associated with the production and disposal of materials.

Various transition metal oxides are being widely used in optoelectronic applications because of their favourable optical and electronic properties. Their unique optical and electronic characteristics make transition metal oxides promising candidates in efficient and sustainable energy conversion systems. One amongst which is tungsten oxide which displays a bandgap ranging from approximately 2.5 to 3.0 eV. This material is responsive to visible light and capable of absorbing light up to around 480 nm [1]. Tungsten oxide (WO_3) stands as a versatile and captivating material in the realm of advanced materials research. It is commonly encountered as an unintentionally doped n-type semiconductor, typically existing in a sub-stoichiometric form like (WO_{3-x}) form i.e.,$WO_{2.9}$, $WO_{2.83}$, etc. Moreover, WO_3 displays the conversion in phase which is as follows: Monoclinic to Orthorhombic at 330°C and Orthorhombic to tetragonal at 710°C [2]. Various methods can be employed for the synthesis of WO_3 nanoparticles including chemical vapour deposition (CVD), sonochemical, sol-gel, hydrothermal, etc [3], [4], [5]. In the form of nanostructures, WO_3 can gain special properties and perform better than when it is in its bulk form. Its unique properties make it a valuable material and hence it is being widely used in electrochromic devices, gas sensing devices, energy storage in batteries and superconductors. $WO_3 \cdot 0.33H_2O$

Researchers have employed various methods to fabricate tungsten oxide and study its properties. Rakhi and Preetha et al. conducted a comparative study on the thermo-chromic capability of $WO_3 \cdot 0.33H_2O$ nanoparticles synthesized through hydrothermal route, both with and without the addition of CTAB surfactants [6]. Kumar et al. fabricated tungsten oxide (WO3) using the acid co-precipitation method, both with and without varying quantities of surfactants (PEG and CTAB) [7].

Despite the numerous studies conducted on the fabrication and properties of tungsten oxide by various researchers, our synthesis endeavours were motivated by the pursuit of specific advancements and unique insights in the field. Our synthesis endeavours were driven by the quest to address specific gaps in the existing knowledge and to offer valuable contributions to the evolving landscape of tungsten oxide applications building upon the foundations laid by previous studies. This research paper aims to thoroughly examine the diverse facets of tungsten oxide, understanding its synthesis route, structural characteristics, and the diverse array of applications.

2. EXPERIMENTAL SECTION

2.1 Chemicals and reagents

Sodium tungstate dehydrate, purified ($Na_2WO_4.2H_2O$; 98.0%) was purchased from M/s Thomas Baker, oxalic acid purified ($(COOH)_2.2H_2O$, 99.5%) and nitric acid (HNO_3; 70%) obtained from M/s CDH Ltd were used during synthesis. Distilled water(resistivity>5MΩ) was obtained from Millipore and used as a solvent during the synthesis. Analytical grade chemicals and reagents were employed for the synthesis of sample without undergoing additional purification.

2.2 Synthesis of WO_3 nanoparticles

Acid co-precipitation method was employed for the synthesis of WO_3 nanoparticles. Initially 0.25 M $Na_2WO_4.2H_2O$ was dissolved in 50 ml distilled water by magnetic stirring for about an hour. Simultaneously, a solution of 0.14 M oxalic acid in 20 ml DI was prepared and kept for stirring. The solution containing oxalic acid was added to the former solution dropwise. After few minutes, a solution containing 5 M HNO_3 was combined with the mixture and stirred at 90°C for 1 hour. The pH of the samples was measured and found to be ~6. Gradually, the solution turned yellowish neon in colour which suggested the formation of precipitate of WO_3. As soon as the precipitate was formed, the solution was left undisturbed for about half an hour. Later, the solution was filtered and washed multiple times with distilled water and ethanol to eliminate impurities. Subsequently, the sample was placed in a vacuum oven, dried at 80°C overnight, and then ground to achieve uniform particles of the WO_3 sample. Fig.1 shows the schematic illustration of the synthesis route.

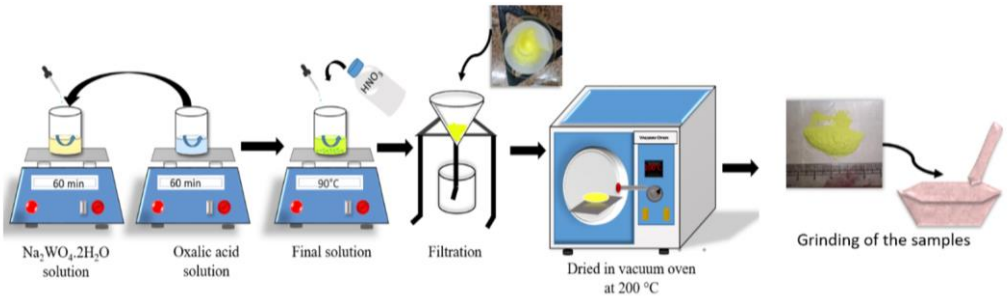

Fig. 1 A schematic illustration depicting the synthesis of WO_3 nanostructures

3. RESULTS AND DISCUSSION

3.1 X-Ray Diffraction

The as-synthesized WO_3 underwent structural analysis using the X-ray Diffraction (XRD) technique, (Panalytical X'pert Pro facility) enabling the investigation of crystalline structure at the atomic and molecular levels. The presence of defects within the material influences the diffraction patterns, introducing imperfections in the crystal structure and microstrain. The XRD data of the as synthesized sample of WO_3 was obtained as shown in fig. 2(a).

The analysis indicated that tungsten oxide exhibits an orthorhombic crystal system, consistent with the data in the JCPDS file 00-018-1418. Additionally, the confirmation of nano-sized particles is achieved by calculating the crystallite size using the Debye-Scherrer equation, yielding values ranging from 7 to 85 nm for individual peaks. The average crystallite size was computed to be 29.36 nm. Furthermore, the XRD data was utilized to estimate various parameters, including dislocation density within the material, microstrain resulting from dislocations and stacking fault. These parameters are determined through specific equations tailored to characterize the structural features of the synthesized nanoparticles [8],[9]. The determination of lattice parameters of the synthesized nanoparticles involved calculating them through the d-spacing values and matching them with the indexed Miller indices, which were then compared with standardized data presented in table 1.

By employing the average crystallite, we determined the dislocation density to be 1.16×10^{-3} nm^{-3} [8]. Therefore, the relatively low dislocation density observed here suggested a more ordered and stable crystal structure of WO_3. Dislocations are linear defects in the crystal structure that can cause lattice distortion, leading to stress and strain in the material. Additionally, microstrain in the sample was calculated by substituting the Full Width at Half Maximum (FWHM) values of individual peaks, yielding a value of 1.96×10^{-3}. The microstrain provides insights into the degree of distortion in the crystal lattice. Furthermore, the stacking fault, a form of planar defect that influences material properties, was found to be 5.94×10^{-3} [8]. These calculated parameters contribute to a comprehensive understanding of the structural characteristics of the WO_3 as shown in table 2.

However, the Debye-Scherrer method, overlooked the impact of material strain on the sample. In order to overcome this constraint and achieve more precise assessments of both crystallite size and the degree of strain within the materials, we employed the Williamson-Hall (W-H) plot as shown in fig. 2(b). In this method, the intercept obtained by W-H plot provided the crystallite size value, determined to be 19.63 nm in this case. Additionally, the strain in the material was derived from the slope of the W-H plot, and in this instance, it was measured as 4.6×10^{-7} as mentioned in table 2.

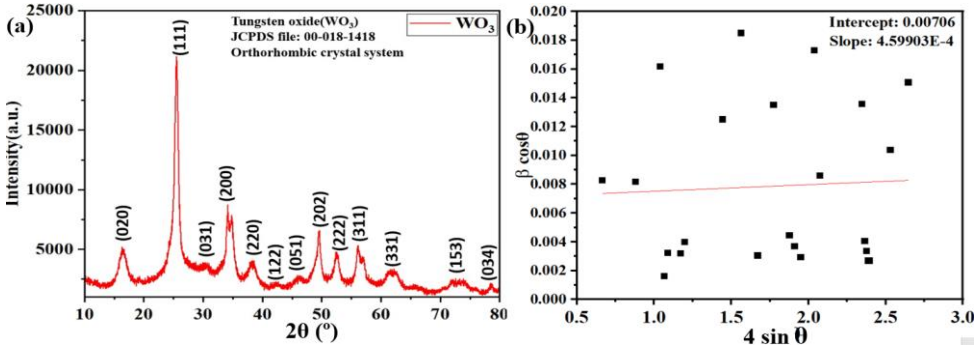

Fig. 2. (a) XRD spectra of the as-synthesized WO_3 (b) Williamson- Hall plot

Table. 1 Comparison of as-calculated lattice parameters with JCPDS database

	a(Å)	b (Å)	c (Å)
JCPDS database value	3.83	7.51	7.28
Calculated value	3.80	7.96	7.07

Table. 2 A summary of calculated structural parameters of WO_3

Parameters	Crystallite size (nm)	Microstrain	Dislocation density (x 10^{-3})	Stacking fault (x 10^{-3})
Debye Scherrer equation	29.36	1.96 x 10^{-3}	1.16	5.94
W- H plot	19.63	4.6 x 10^{-7}	-	-

3.2 UV-Vis Spectroscopy

UV-Visible (UV-Vis) spectroscopy has emerged as a powerful analytical technique and has been used to obtain and showcase the optical and electronic properties of tungsten oxide (WO_3). In this study, the UV-vis absorbance data was obtained with the help of (make: Shimadzu, model: 2600i) spectrophotometer. The absorbance data for tungsten oxide, as illustrated in Fig. 3(a), revealed maximum peaks at wavelengths of 196 nm, 223 nm, 300 nm, 347 nm, and 376 nm for the sample. Notably, the sample exhibited significant absorbance in the UV region, and this absorbance is observed to increase at higher wavelengths. This data was further used to estimate the optical properties such as the energy band gap, refractive index and the HOMO and LUMO levels of the material. The UV-Vis spectra were analyzed using the Kubelka-Monk function (F(R∞)), which was subsequently derived from the UV-Vis DRS absorbance data. The direct band gap (E_g) was obtained with the help of tauc's plot plotted between $(\alpha h\upsilon)^2$ and $h\upsilon$ illustrated in fig. 3 (b) and by extrapolating the linear portion of the plot the band gap for the sample was calculated [10], [11], [12]. The band gap so obtained was 2.5 eV.

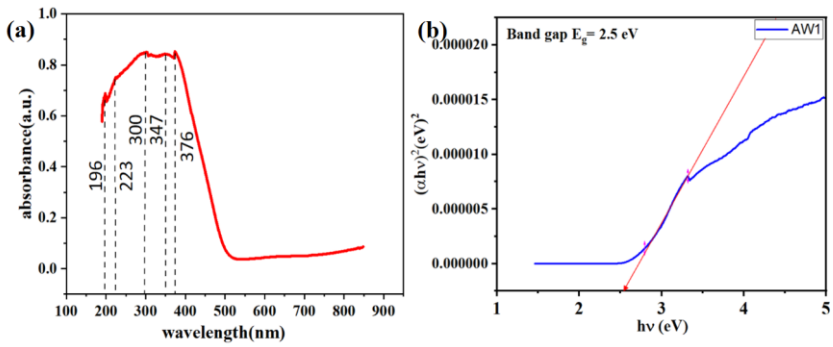

Fig. 3. (a) Absorbance spectra (b) Tauc plot of the as- synthesized sample

The refractive index (n) of the as- synthesized material is related to its optical properties and is used to estimate the refractive index directly from band gap data [13], [14]. Substituting the values of band gap we obtained the refractive index for the sample as 2.56.

The HOMO (Highest Occupied Molecular Orbital) and LUMO (Lowest Unoccupied Molecular Orbital) levels are associated with the molecular orbitals of a compound and thereby producing changes in electron occupancy between these orbitals which give rise to absorption bands observed in the UV-Vis spectrum. In this study, the UV- vis spectra obtained was further used for estimating the valence bands and conduction bands i.e. the HOMO and LUMO levels for the sample [15], [16].The valence and conduction band were obtained at 3.34 eV and 6.14 eV.

3.3 Scanning Electron Microscopy

The surface morphology of the as- synthesized sample was examined at appropriate locations and magnifications utilizing a Zeiss Gemini SEM 500, a field emission type scanning electron microscope (FESEM) with an operational acceleration voltage of 20 kV. Fig. 4(a,b) showed the surface morphology of WO_3. At high magnification, the morphology of WO_3 revealed the presence of nanosheets that intricately assembled to create nanoflowers, demonstrating a configuration devoid of agglomeration. Surface energy influenced the tendency of particles to form specific structures and forming organized assembly of nanosheets into nanoflowers

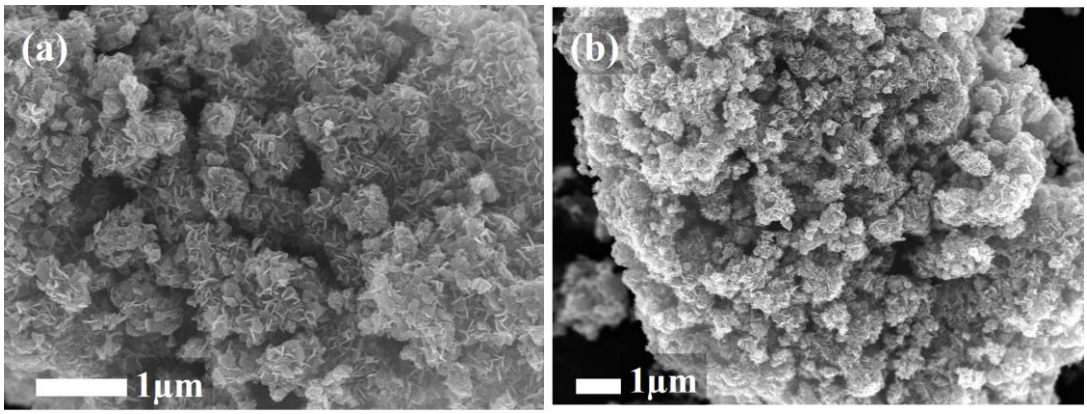

Fig. 4. (a,b) FESEM images of WO_3 nanostructures

The morphology of nanosheets and assembled nanoflowers has high aspect ratio which makes the material a potential candidate to be used as a photocatalyst in various applications like degradation of organic pollutants in waste water management, hydrogen evolution reaction, oxygen evolution reaction, etc.

4. CONCLUSION

Nanostructure of tungsten oxide (WO_3) were prepared by an economically viable and environmentally friendly approach involving acid co-precipitation. The XRD analysis verified that the synthesized sample predominantly exhibited the monoclinic phase. The crystallite size of the as synthesized sample was found to be 29.36 nm. Furthermore, the optical investigation has demonstrated that WO_3 is a promising material for applications in various fields, attributable to its relatively lower optical band gap, specifically 2.5 eV. The examination of WO_3 surface morphology through Field Emission Scanning Electron Microscopy (FESEM) uncovered the existence of nanosheets intricately arranged to form nanoflowers. This arrangement showcased a configuration without any agglomeration.

ACKNOWLEDGEMENTS

The authors express their gratitude to Prof. Anand Srivastava, Vice-Chancellor of Netaji Subhas University of Technology, Delhi, for providing the necessary resources essential for conducting the research.

FUNDING

This research work did not receive any financial support from any organization.

CONFLICTS OF INTEREST

The authors have no conflicts of interest to declare.

REFERENCES

1. P. Dong, G. Hou, X. Xi, R. Shao, and F. Dong, "WO3-based photocatalysts: morphology control, activity enhancement and multifunctional applications," *Environ. Sci. Nano*, vol. 4, no. 3, pp. 539–557, 2017, doi: 10.1039/C6EN00478D.
2. S. B. Upadhyay, R. K. Mishra, and P. P. Sahay, "Cr-doped WO3 nanosheets: Structural, optical and formaldehyde sensing properties," *Ceram. Int.*, vol. 42, no. 14, pp. 15301–15310, Nov. 2016, doi: 10.1016/J.CERAMINT.2016.06.170.
3. N. Shankar, M. F. Yu, S. P. Vanka, and N. G. Glumac, "Synthesis of tungsten oxide (WO3) nanorods using carbon nanotubes as templates by hot filament chemical vapor deposition," *Mater. Lett.*, vol. 60, no. 6, pp. 771–774, Mar. 2006, doi:

10.1016/J.MATLET.2005.10.009.

4. M. Aliannezhadi, M. Abbaspoor, F. Shariatmadar Tehrani, and M. Jamali, "High photocatalytic WO3 nanoparticles synthesized using Sol-gel method at different stirring times," *Opt. Quantum Electron.*, vol. 55, no. 3, Mar. 2023, doi: 10.1007/S11082-022-04540-8.
5. C. M. Wu, S. Naseem, M. H. Chou, J. H. Wang, and Y. Q. Jian, "Recent advances in tungsten-oxide-based materials and their applications," *Front. Mater.*, vol. 6, Mar. 2019, doi: 10.3389/FMATS.2019.00049.
6. C. Rakhi and K. C. Preetha, "Thermal treatment effects on tungsten oxide nanostructures synthesized by hydrothermal method," *Appl. Phys. A Mater. Sci. Process.*, vol. 128, no. 12, Dec. 2022, doi: 10.1007/S00339-022-06223-3.
7. T. Kumar, Shreya, P. Phogat, V. Sahgal, and R. Jha, "Surfactant-mediated modulation of morphology and charge transfer dynamics in tungsten oxide nanoparticles," *Phys. Scr.*, vol. 98, no. 8, Aug. 2023, doi: 10.1088/1402-4896/ACE566.
8. S. Sharma, P. Phogat, R. Jha, and S. Singh, "Electrochemical and Optical Properties of Microwave Assisted MoS2 Nanospheres for Solar Cell Application," *Int. J. Smart Grid Clean Energy*, pp. 66–72, 2023, doi: 10.12720/SGCE.12.3.66-72.
9. A. Sharma, Shreya, P. Phogat, R. Jha, and S. Singh, " Hydrothermally Synthesized NiS 2 and NiSO 4 (H 2 O) 6 Nanocomposites and its Characterizations ," *MATEC Web Conf.*, vol. 393, p. 01016, 2024, doi: 10.1051/MATECCONF/202439301016.
10. J. Dahiya, P. Phogat, A. Hooda, and S. Khasa, "Investigations of Praseodymium doped LiF-ZnO-Bi2O3-B2O3 glass matrix for photonic applications," p. 020065, 2024, doi: 10.1063/5.0178197.
11. P. Phogat, Shreya, R. Jha, and S. Singh, "Optical and Microstructural Study of Wide Band Gap ZnO@ZnS Core–Shell Nanorods to be Used as Solar Cell Applications," *Lect. Notes Mech. Eng.*, pp. 419–429, 2023, doi: 10.1007/978-981-99-2349-6_38.
12. Shreya, P. Phogat, S. Singh, and R. Jha, " Reduction mechanism of hydrothermally synthesized wide band gap ZnWO 4 nanorods for HER application ," *MATEC Web Conf.*, vol. 393, p. 01004, 2024, doi: 10.1051/MATECCONF/202439301004.
13. Shreya, P. Phogat, R. Jha, and S. Singh, "Elevated Refractive Index of MoS2 Amorphous Nanoparticles with a Reduced Band Gap Applicable for Optoelectronics," *Lect. Notes Mech. Eng.*, pp. 431–439, 2023, doi: 10.1007/978-981-99-2349-6_39.
14. P. Phogat, Shreya, R. Jha, and S. Singh, "Phase Transition of Thermally Treated Polyhedral Nano Nickel Oxide with Reduced Band Gap," *MATEC Web Conf.*, vol. 393, p. 01001, 2024, doi: 10.1051/MATECCONF/202439301001.
15. A. Rai, P. Phogat, Shreya, R. Jha, and S. Singh, "Microwave Assisted Zinc Sulphide Quantum Dots for Energy Device Applications," *MATEC Web Conf.*, vol. 393, p. 01011, 2024, doi: 10.1051/MATECCONF/202439301011.
16. S. Rai, Shreya, P. Phogat, R. Jha, and S. Singh, " Hydrothermal synthesis and characterization of selenium-doped MoS 2 for enhanced optoelectronic properties ," *MATEC Web Conf.*, vol. 393, p. 01008, 2024, doi: 10.1051/MATECCONF/202439301008